JOURNAL OF VIROLOGY, Nov. 2003, p. 12232–12242 Vol. 77, No. 22
0022-538X/03/$08.00+0 DOI: 10.1128/JVI.77.22.12232–12242.2003

Neuroadapted Yellow Fever Virus 17D: Determinants in the Envelope Protein Govern Neuroinvasiveness for SCID Mice

Michael Nickells and Thomas J. Chambers*

Department of Molecular Microbiology and Immunology, St. Louis University Health Sciences Center, St. Louis, Missouri 63104

Received 28 May 2003/Accepted 13 August 2003

A molecular clone of mouse-neuroadapted yellow fever 17D virus (SPYF-MN) was used to identify critical determinants of viral neuroinvasiveness in a SCID mouse model. Virus derived from this clone differs from nonneuroinvasive YF5.2iv virus at 29 nucleotide positions, encoding 13 predicted amino acid substitutions and 2 substitutions in the 3′ untranslated region (UTR). The virulence determinants of SPYF-MN for SCID mice were identified by constructing and characterizing intratypic viruses in which the E protein of SPYF-MN was expressed in the YF5.2iv background (SPYF-E) or the E protein of YF5.2iv was expressed in the SPYF-MN background (YF5.2-E). SPYF-E caused lethal encephalitis in young adult SCID mice after intraperitoneal inoculation, with average survival times and tissue virus burdens resembling those of mice inoculated with the parental SPYF-MN virus. To define which domains of the E protein are involved in neuroinvasiveness, two viruses were tested in which the amino acid substitutions in domains I-II and III were segregated. This revealed that substitutions in domain III (residues 305, 326, and 380) were critical for the neuroinvasive phenotype, based on average survival times and tissue burdens of infectious virus. Comparison of growth properties of the various intratypic viruses in cell culture indicated that no inherent defects in replication efficiency were likely to account for the biological differences observed in these experiments. These findings demonstrate that the E protein is a critical factor for yellow fever virus neuropathogenesis in the SCID mouse model and that the neuroinvasive properties depend principally on functions contributed by domain III of this protein. To assess whether critical determinants for neuroinvasion of normal ICR mice by SPYF virus were also in the E protein, sequences of viruses recovered from brains of ICR mice succumbing to encephalitis with the parental SPYF virus were derived. No differences were found in the E protein; however, two substitutions were present in the 3′ UTR compared to that of SPYF-MN, one of which is predicted to alter RNA secondary structure in this region. These findings suggest that the 3′ UTR may also affect neuroinvasiveness of SPYF virus in the mouse model.

Yellow fever virus (YFV), the prototype member of the *Flavivirus* genus, exhibits neurovirulence in rodent and primate hosts. Acute encephalitis is a recognized complication of human vaccination against yellow fever, having been encountered in association with the French neurotropic vaccine, but only rarely with the 17D strain, and usually in young children (13). Different strains of YFV can be distinguished by their levels of mouse neurovirulence (4, 12, 21, 42, 43), and this virulence property can be enhanced by serial passage of the virus in the mouse brain (9, 30, 45, 47). Genetic analyses of flaviviruses which differ in neurovirulence properties have identified mutations in numerous regions of the viral genome. However, mutations in the viral envelope (E) protein are generally regarded as having the most important effects on virulence (reviewed in reference 29). For instance, nucleotide sequence analysis of the E protein of the French neurotropic virus (Institut Pasteur) strain of YFV revealed a total of 25 nucleotide (nt) substitutions relative to the attenuated 17D-204 vaccine, with 17 amino acid substitutions (17, 50). Furthermore, in the case of a neurovirulent revertant of the YFV 17D vaccine, two mutations were found within the E region of the viral genome (18). Although the molecular mechanisms associated with the pathogenesis of encephalitis due to YFV have not been well characterized, mutations in the E protein are likely to contribute to this process by governing efficiency of virus attachment and entry into host cells and spread through critical target tissues. This conclusion is based on collective studies of other flaviviruses (5, 24, 27, 28, 33, 34, 42, 43). Less is known about the effects of neurovirulence determinants in the nonstructural and untranslated regions (UTRs) of the flavivirus genome (6, 11, 19, 23, 31, 35). Mutations in these regions could affect virulence by altering the efficiency of viral replication through deleterious effects on enzymatic activities involved in viral RNA transcription or on the RNA structures required for binding to host and viral proteins that participate in transcription and/or translation.

In a previous study, the mouse neurovirulence of a neuroadapted strain of YFV 17D (SPYF) was characterized, and a molecular clone of this virus (SPYF-MN) was engineered (8). Virus derived from this clone was found to be neuroinvasive for young adult SCID mice and had measurably higher neurovirulence for normal mice than nonneuroadapted YF5.2iv virus, which represents the YFV 17D strain (41). A total of 29 nt substitutions differentiated these two viruses, encoding 13 amino acid substitutions in the E, NS1, NS2A, NS4, and NS5 regions, and 2 nucleotide substitutions in the 3′ UTR. To further investigate the genetic basis for the neurovirulence phenotype of the SPYF-MN virus, we constructed intratypic viruses between SPYF-MN and YF5.2iv in which the E protein

* Corresponding author. Mailing address: Department of Molecular Microbiology and Immunology, St. Louis University Health Sciences Center, 1402 South Grand Ave., St. Louis, MO 63104. Phone: (314) 577-8447. Fax: (314) 773-3403. E-mail: chambetj@slu.edu.

of each virus was exchanged into the genetic background of the other and tested their virulence properties in the SCID mouse model. These studies revealed that the E protein of the SPYF-MN virus was critical for neuroinvasion. Testing of other subdomain intratypic viruses containing exchanges of domains I-II and III of the SPYF-MN and YF5.2iv E proteins indicated that amino acid substitutions in domain III of the SPYF-MN E protein were sufficient to generate the neuroinvasive phenotype. This model may be useful for evaluating mutations involved in neuropathogenesis of YFV that are below the levels detectable by conventional methods such as experimentation in normal mice or monkey neurovirulence testing. Data from such studies might be used in support of acceptable attenuation phenotypes of live-attenuated flavivirus vaccine candidates derived by genetic engineering.

MATERIALS AND METHODS

Cells and viruses. Vero and BHK-21 cells were grown at 37°C in alpha minimal essential medium (alpha-MEM) supplemented with 10% fetal bovine serum. The neuroadapted SPYF-MN virus clone and YF5.2iv virus generated from a YFV 17D molecular clone have been described previously (8). Plaque assays for virus quantitation were routinely done in Vero cells as previously described (49). Viruses were diluted in phosphate-buffered saline (PBS) plus 10% fetal bovine serum for inoculation of mice.

Mouse experiments. Mice used for these experiments were SCID/ICR mice (Taconic, Germantown, N.Y.). Mice were inoculated between 4 and 5 weeks of age for studies of neuroinvasiveness. They were housed in microisolator units and handled under sterile conditions during experimental manipulations. Mice were inoculated by the intraperitoneal (i.p.) route for peripheral inoculation, observed until the onset of a moribund condition, and then sacrificed in accordance with guidelines of the Institutional Animal Care and Use Committee. Statistical analyses of differences in mortality were done with Fisher's exact test. Differences in average survival times were analyzed with the Mann-Whitney test (two-sided). For analysis of virus content in tissues of infected mice, tissues were recovered by dissection after perfusion with PBS at 4°C and stored at −70°C until used for virus quantitation. Titration of tissue-associated virus was done by preparing 10% suspensions of tissue homogenates in a Dounce homogenizer in PBS plus 10% fetal bovine serum and by performing plaque assays of diluted samples on Vero cells. Plaque assays were done on cell monolayers under 1.0% ME agarose (SeaKem) in alpha-MEM plus 5% fetal bovine serum. Plaques were visualized by staining after 6 to 7 days with 0.05% neutral red in PBS and then were counted after fixation in 10% formalin and staining with crystal violet.

Nucleotide sequencing of viruses. To verify the sequences of the intratypic viruses constructed for these experiments, RNA was prepared from monolayers of Vero cells infected during amplification of the viruses used for studies of mouse neuroinvasiveness. RNA was isolated with TRIzol (Gibco/BRL), reverse transcribed with Superscript II (Gibco/BRL), and used for synthesis of PCR fragments which spanned the YFV genome using previously described methods (8). PCR fragments were cloned into pZeroBlunt-TOPO, and multiple clones for each amplicon were sequenced across regions containing the predicted nucleotide substitutions of the intratypic virus clones, as described in more detail below.

In experiments to determine the nucleotide sequence of brain-associated YFV, RNA was prepared from brains of mice infected with SPYF virus at the time of onset of a moribund condition. RNA was extracted and used for reverse transcription (RT)-PCR as described above, except that most PCR products were reamplified with a second set of nested primers as described below. The reverse primers used for first-strand cDNA synthesis were as follows: YF2486(−), 5′-GATACCATTTCCGCACTTGAGCTC-3′ (nt 2509 to 2486); YF2980(−), 5′-GTGTATTCAAAGACTGCGTCCATG-3′ (nt 2979 to 2956); YF5300(−), 5′-GCCAACACAAGAGTGCGCAAGCG-3′ (nt 5250 to 5228); YF6210(−), 5′-GGCAGGTCACAATTCCTCA-3′ (nt 6210 to 6192); YF8300(−), 5′-GGCTCCAGACACGTAGTAC-3′ (nt 8311 to 8293); YF9766(−), 5′-CATGGAAGTGGTGGGAACAGAAGGGC-3′ (nt 9791 to 9766); and YF10862(−), 5′-GGAAACCTACTGTTTGTGTTTTGGTG-3′ (nt 10861 to 10836).

The PCR primer pairs used to generate nested PCR products for sequencing were as follows. For first-strand cDNA from YFV 2486(−), the forward primer was 5′-GAGTAAATCCTGTGTGCTAATTG-3′ and the reverse primer was 5′-ATTTGTGTCCTTTGTAACCCTCAT-3′ (region amplified, nt 1 to 1780). For first-strand cDNA from YFV 2980(−), the forward primer was 5′-GGAAGAATGGGTGAAAGGC-3′ and the reverse primer was 5′-GTGTATTCAAAGACTGCGTCCATG-3′ (region amplified, nt 812 to 2979); the forward nested primer was 5′-GACGCAATGAGTCGTGATTGCCC-3′ and the reverse nested primer was 5′-GATACCATTTCCGCACTTGAGCTC-3′ (region amplified, nt 919 to 2509). For first-strand cDNA from YFV 5300(−), the forward primer was 5′-GGTAGGAGTGATCATGAT-3′ and the reverse primer was 5′-GATGTTCACATTCCTCGATGATC-3′ (region amplified, nt 2410 to 4628); the forward nested primer was 5′-GGTAGGAGTGATCATGAT-3′ and the reverse nested primer was 5′-GCTAACCAGCATCATCAGG-3′ (region amplified, nt 2410 to 4309). For first-strand cDNA from YFV 6210(−), the forward primer was 5′-CTTGTGCTGACCCTAGGA-3′ and the reverse primer was 5′-GCCCTTTTATTGCCACCTTCCTCCC-3′ (region amplified, nt 3812 to 5918); the forward nested primer was 5′-CTGTGTGCATTTCTGGCAACC-3′ and the reverse nested primer was 5′-TTACGCAAAGAGGCAGCCA-3′ (region amplified, nt 4142 to 5715). For first-strand cDNA from YFV 8300(−), the forward primer was 5′-GCCTGGGACTAGTGATGAA-3′ and the reverse primer was 5′-TTCCCTCTTGCAGACTTCACCC-3′ (region amplified, nt 5540 to 7681); the forward nested primer was 5′-TCCATCCATCAGAGCTGC-3′ and the reverse nested primer was 5′-TTCCCTCTTGCAGACTTCACCC-3′ (region amplified, nt 5671 to 7681). For first-strand cDNA from YFV 9766(−), the forward primer was 5′-TTGGCTGAAGGCATTGTC-3′ and the reverse primer was 5′-GCCACATATACCATATGGCACGGC-3′ (region amplified, nt 7463 to 9074); the forward nested primer was 5′-TTGGCTGAAGGCATTGTC-3′ and the reverse nested primer was 5′-CAGCTTCTTCTCTCTTTTCCCC-3′ (region amplified, nt 7463 to 9025). For first-strand cDNA from YFV 10862(−), the forward primer was 5′-CCCCTTTTGGACAGCAAAGAGTG-3′ and the reverse primer was 5′-GATACCATTTCCGCACTTGAGCTC-3′ (region amplified, nt 8679 to 10861); the forward nested primer was 5′-CTGGACAGAGAAAAGAACCCC-3′ and the reverse nested primer was 5′-GATACCATTTCCGCACTTGAGCTC-3′ (region amplified, nt 8792 to 10861).

The cDNA products were subjected to PCR amplification with Deep Vent DNA polymerase (New England Biolabs), typically using amplification cycles of 2 min of denaturation, 1 min of annealing (55°C), and extension for up to 2.5 min. PCR products were isolated by agarose gel electrophoresis, purified with Wizard PCR preps (Promega), and used for direct sequencing. Nucleotide sequencing was done with DTCS Quick Start reagents (Beckman Coulter) and analyzed on an Applied Biosystems DNA sequencer. All chromatograms were also analyzed manually to detect and verify any nucleotide substitutions.

Construction of intratypic viruses. The SPYF-MN (8) and YF5.2iv (41) molecular clones were used as starting materials for construction of intratypic viruses. Both of these clones are based on a two-plasmid system for assembly of DNA templates for transcription of infectious viral RNA. pYF5′3′IV contains YFV nucleotide sequences from nt 1 to 2271 and 8275 to 10862 (YFV numbering) downstream of an SP6 promoter, and pYFM5.2 contains the YFV sequence from nt 1363 to 8704. The intratypic virus clones YF5.2-E and SPYF-E were constructed by modifying pYF5′3′IV and pYFM5.2 containing YF5.2iv or SPYF-MN sequences. pYF5′3′IV containing the YF5.2iv E region was used for construction of YF5.2-E, since there are no differences in the nucleotide sequences of SPYF-MN and YF5.2iv upstream of the E protein (8). The SPYF-MN E sequence was introduced into the plasmids from pZeroBlunt-TOPO (Invitrogen) clones containing these sequences (8). The plasmids used for the construction of SPYF-E virus were constructed as follows. pYF5′3′IV was digested with *Sal*I and *Xho*I and religated to form the plasmid pYF5′3′IV-del(*Sal*I/*Xho*I). This construct lacks YF5.2iv sequence from nt 9423 to 10862 and was digested with *Ava*I and *Nsi*I to excise the YF5.2iv sequence from nt 536 to 1655. This *Ava*I/*Nsi*I deletion was restored using the *Ava*I/*Nsi*I fragment derived from digestion of pZeroBlunt containing SPYF-MN nt 423 to 2503. The excised *Sal*I/*Xho*I fragment was then restored by replacing the *Nsi*I/*Not*I fragment of this construct (nt 1655 to 6675[vector]) with the pYF5′3′IV fragment derived by digestion with the same endonucleases. The resultant complete pYF5′3′IV plasmid contains the SPYF-MN sequence from nt 536 to 1655 (YFV numbering).

The pYFM5.2 plasmid was digested with *Sac*I to excise two fragments (nt 2486 to 4334 and 4334 to 5108) and religated to form pYFM5.2-del(*Sac*I). This plasmid was then digested with *Nsi*I and *Sac*I to delete the YF5.2iv sequence from nt 1655 to 2486, which was restored with the corresponding fragment from pZeroBlunt TOPO containing SPYF nt 424 to 2503. The *Sac*I deletion was then restored by ligation of the pYFM5.2-derived partial *Sac*I digestion product (nt 2486 to 5108) into the *Sac*I site of pYFM5.2-del(*Sac*I) plasmid containing SPYF-MN nt 1655 to 2486. The full-length template for synthesis of RNA transcripts was prepared by digesting both pYF5′3′IV and pYFM5.2 with *Nsi*I and *Aat*II, ligating the nt 1655 to 8402 fragment from pYFM with the pYF5′3′IV fragment lacking this sequence, digesting the ligation product with *Xho*I to linearize the plasmid at the 3′ terminus of the YFV sequence (nt 10862), and

generating RNA transcripts by runoff transcription as previously described (41). Vero cells were then transfected with approximately 100 ng of RNA transcript to generate live virus. Virus yields were quantitated by plaque assay on Vero cells as described above.

The plasmids used for the construction of the SPYF-E_{I-II} and SPYF-E_{III} viruses were the same as those described above. For the production of SPYF-E_{I-II}, the *Nsi*I/*Aat*II fragment of pYF5′3′IV containing SPYF-MN nt 536 to 1655 was ligated to the *Nsi*I/*Aat*II fragment of pYFM5.2IV. For the production of SPYF-E_{III}, the *Nsi*I/*Aat*II fragment of pYFM5.2 containing SPYF-MN nt 1655 to 2486 was ligated to the *Nsi*I/*Aat*II fragment of pYF5′3′IV.

The pYF5′3′IV and pYFM5.2 plasmids used for construction of YF5.2-E were constructed as follows. pYF5′3′IV was digested with *Bsm*I to delete the fragment from nt 459 to 1514 and religated to form pYF5′3′IV-del(*Bsm*I). This plasmid was then digested with *Nde*I and *Xba*I to excise the fragment from nt 9058 to 10708, which was replaced with the equivalent SPYF-MN sequence derived from a pZeroBlunt-TOPO clone containing SPYF-MN nt 9051 to 10862. To restore the deleted *Bsm*I fragment, this plasmid was digested with *Eco*RI and *Xba*I and the resultant fragment (nt 8255 to 10708) was ligated into pYF5′3′IV digested with the same enzymes. The resultant pYF5′3′IV contains SPYF-MN nt 9058 to 10708. pYFM5.2 containing SPYF-MN nt 2486 to 5108, 5459 to 6797, and 7444 to 8027 was constructed in four steps. SPYF-MN nt 2486 to 5108, derived from a pZeroBlunt-TOPO clone containing SPYF-MN nt 2482 to 5250, was ligated as a partial *Sac*I digestion product into pYFM5.2-del(*Sac*I) (described above). The preparation of a separate pYFM5.2 containing SPYF-MN nt 5459 to 6701 and 7444 to 8027 was previously described (8). Both of these plasmids were digested with *Nsi*I and *Nhe*I, and the appropriate fragments (nt 1655 to 5459, respectively), were ligated to generate pYFM5.2 containing SPYF-MN nt 2486 to 5108, 5459 to 6701, and 7444 to 8027. To introduce the SPYF-MN substitution at nt 6758, this plasmid and pYFM5.2 containing SPYF-MN nt 1655 to 5108, 5459 to 6797, and 7444 to 8027 (prepared as described previously) were both digested with *Ava*I. The 3,801- to 6,797-nt fragment from the plasmid containing SPYF-MN nt 5459 to 6797 was ligated into the *Ava*I site of the other plasmid to generate the desired pYFM5.2 construct. This plasmid and the pYF5′3′IV containing SPYF-MN nt 9058 to 10708 were used to produce full-length templates by *Nsi*I/*Aat*II digestion and assembly of transcription templates as described above.

To confirm the presence of the SPYF-MN substitutions in the SPYF-E and YF5.2-E viruses, total RNA was purified from Vero cells transfected with infectious RNA, and regions containing the predicted substitutions in each virus were amplified by RT-PCR using previously described primer pairs (8). PCR products were ligated into pZeroBlunt-TOPO vectors and used to transform Top 10 *Escherichia coli* cells (Invitrogen) as previously described (8). Five to six clones from each PCR product were sequenced, and all contained the predicted SPYF-MN substitutions. However, two of the six SPYF-E-derived clones containing nt 424 to 2503 had additional substitutions. In one clone, a C (nt 1172) was changed to A, resulting in replacement of histidine (residue 67 of the E protein) with asparagine, and a silent substitution of A to G occurred at nt 2152. In another clone, a C (nt 1147) was changed to A, resulting in replacement of leucine (residue 159 of the E protein) with isoleucine. Of five YF5.2-E-derived clones containing nt 3476 to 5250, in one clone a C (nt 4872) was changed to T, resulting in replacement of alanine (residue 101 of the NS3 protein) with valine. In one of six YF5.2-E-derived clones containing nt 9051 to 10861, a C (nt 10029) was changed to T, resulting in replacement of threonine (residue 798 of NS5) with isoleucine, and an A (nt 10475) in the 3′ UTR was changed to G.

The YF5.2iv, SPYF-MN, SPYF-E_{I-II}, and SPYF-E_{III} viruses were plaque purified twice from Vero cells, with intervening amplification on SW13 cells. The resultant virus stocks were amplified one additional time on Vero cells, total RNA was isolated, and the envelope gene was amplified by RT-PCR. PCR products were ligated into pZeroBlunt-TOPO, and three clones from each PCR were sequenced. All viruses contained the expected sequence through the E region. In addition, one clone from SPYF-E_{I-II} contained a silent substitution, A (nt 1233) to G (glycine residue at position 87 of the E protein), but no other substitutions were detected. The primer pair used to amplify the E regions of SPYF-E_{I-II} and SPYF-E_{III} was as follows: forward primer, 5′-GGAAGAATGG GGTGAAAGGC-3′; reverse primer, 5′-GATACCATTTCCGCACTTGAGCT C-3′ (amplifies the regions from nt 812 to 2509).

Virus growth curves. Viruses were inoculated onto monolayers of BHK cells in six-well Costar plates at 37°C in triplicate at a multiplicity of infection of 0.001 PFU/cell. Media were harvested at 12, 24, 36, 48, and 84 h postinfection, followed by replacement with fresh medium. The virus yields were determined by plaque assay on Vero cells.

Molecular modeling. A homology model for the YFV 17D E protein was generated based on the structure for the soluble fragment of the E protein of tick-borne encephalitis virus (39). The amino acid sequence of the YF5.2iv virus E protein was submitted to the automated comparative protein modeling server Swiss-Model via the ExPASy web server for homology modeling by the first-approach mode. The crystal structure of the soluble ectodomain of the tick-borne encephalitis virus E protein (ExPDB template code 1 svb) was used as the modeling template. Sequence alignment was determined by Swiss-Model, which aligned amino acids 1 to 384 of the YF5.2iv E protein sequence with those of tick-borne encephalitis virus E protein. Rotamers for amino acid substitutions in domain III of YFV were compared for prediction of the most favorable energy configuration of the side chains using the Swiss-PdbViewer.

RNA structures were generated with RNA mfold, version 3.1 (26, 51). The region from the end of the open reading frame up to but not including the 3′-terminal stem loop was analyzed, based on the absence of any substitutions in the latter region and the predicted stable structure for these terminal 180 nt. Folding constraints were used to yield a structure for YF5.2iv that conformed to optimized predicted structures for the 3′ UTR (36, 37, 38). Several structures with similar energies were examined for each virus (YF5.2iv, SPYF-MN, and SPYF).

RESULTS

Construction of intratypic YF5.2iv and SPYF viruses. Figure 1 illustrates the structure of the various viruses used in the experiments for this study. The YF5.2iv and SPYF-MN viruses were used as controls. The E protein of the SPYF virus (SPYF-MN molecular clone) differs from that of YF5.2iv virus by the following five amino acid substitutions: glycine for arginine at position 52 (domain I), threonine for isoleucine at position 173 (domain II), valine for phenylalanine at position 305 (domain III), glutamate for lysine at position 326 (domain III), and threonine for arginine at position 380 (domain III) (Table 1). To verify that the viruses used in the experiments did contain the expected engineered mutations, RT-PCR was used to derive fragments covering the entire genome, and multiple plasmid clones containing the corresponding PCR fragments were sequenced for each virus, as described in Materials and Methods. Using this approach, we confirmed that the expected residues were present at the relevant genetic loci, and only minor variants, containing very rare mutations, were present in the virus stocks.

The parental YF5.2iv and SPYF-MN viruses could be readily distinguished from one another by their plaque sizes. YF5.2iv formed larger plaques (5 mm) than SPYF-MN (1 mm) on Vero cells (Fig. 1 and 2). The SPYF-E virus exhibited a plaque size similar to that of SPYF-MN, indicating that the E protein apparently governs the small plaque phenotype of the latter virus. Furthermore, comparison of the plaque sizes of the domain-intratypic viruses revealed that the SPYF-E_{III} virus formed small plaques, whereas SPYF-E_{I-II} formed plaques that were similar in size to those of YF5.2iv virus. This indicates that domain III within the SPYF E protein in fact governs the small plaque size of the SPYF-MN and SPYF-E viruses.

Growth efficiency of intratypic viruses in cell culture. To verify that the engineered viruses did not exhibit any major defects in their replication efficiencies that might affect comparisons of their virulence properties in mice, their growth kinetics were analyzed in BHK cells (Fig. 3). After a very low multiplicity of infection in this cell line, YF5.2iv virus grew to a titer of nearly 6 log (PFU/ml) by 48 h. Both YF5.2iv-E and SPYF-E_{I-II} viruses, which contain the E protein of YF5.2iv virus or its domain III only, respectively, exhibited replication efficiencies that were generally similar to that of YF5.2iv, ex-

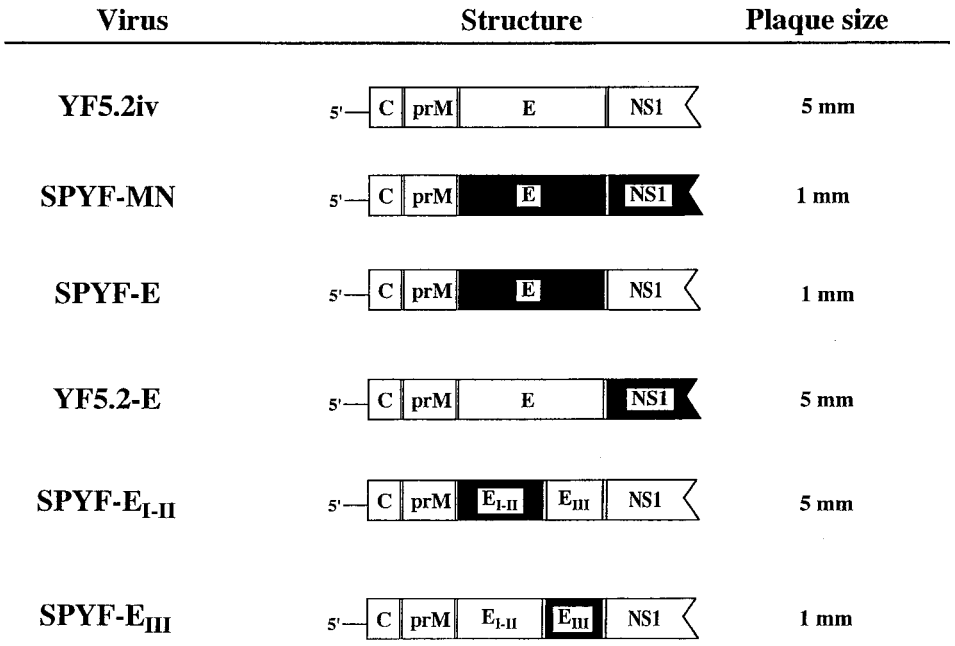

FIG. 1. Structure of parental and intratypic viruses. Top panels, YFV genomes for the YF5.2iv and SPYF-MN molecular clones; middle panels, genomes of the intratypic SPYF-E and YF5.2iv-E viruses; bottom panels, domain-intratypic SPYF-E_{I-II} and SPYF-E_{III} viruses. Shaded areas indicate the regions of SPYF-MN sequence, and open areas indicate regions of YF5.2iv sequence. The genomes are truncated within the NS1 region for the sake of clarity. Plaque sizes from plaque assays on Vero cells are indicated.

cept the yields of the latter viruses were slightly greater than that of YF5.2iv over the initial 36 h postinfection. In contrast, SPYF-MN virus replicated less efficiently over the interval examined, reaching a maximum titer of approximately 5 log (PFU/ml) by 84 h postinfection. The SPYF-E and SPYF-E_{III} viruses exhibited replication efficiencies similar to that of SPYF-MN. These data indicate that domain III of the SPYF virus confers a reduced replication efficiency upon YFV during low-multiplicity infection of BHK cells.

Neuroinvasiveness of SPYF-E and YF5.2-E viruses. To determine if the E protein is the dominant factor controlling the virulence properties of the SPYF-MN virus in SCID mice, the SPYF-E and YF5.2-E viruses were compared to the parental SPYF-MN and YF5.2iv viruses for neuroinvasiveness. Groups of SCID/ICR mice were subjected to i.p. inoculation with 5×10^5 PFU of the respective viruses. Results are shown in Fig. 4. Consistent with previous results (8), the SPYF-MN virus caused fatal encephalitis in all mice, with an average survival time of 17.6 days (range, 11 to 24 days). In contrast, the YF5.2iv virus did not cause any mortality over 20 weeks in these experiments, and the mice did not exhibit any signs of illness. The SPYF-E virus was similar to the SPYF-MN virus, as it caused 100% mortality in mice, with an average survival time of 20.2 days (range, 10 to 30 days). This survival time was somewhat longer than that associated with the SPYF-MN virus, but the difference was not significant. In contrast to this result, the virulence of YF5.2-E virus resembled that of the YF5.2iv virus, since it did not cause any mortality in mice over the period of observation of these experiments. These results indicate that the neuroinvasiveness of SPYF-MN virus for SCID mice is governed by determinants within the SPYF E

TABLE 1. Amino acid substitutions in E proteins

Virus	Amino acid at Envelope domain and position				
	II	I	III		
	52	173	305	326	380
YF5.2iv	R	I	F	K	R
YF5.2iv-E	R	I	F	K	R
SPYF-MN	G	T	V	E	T
SPYF-E	G	T	V	E	T
SPYF-E_{III}	R	I	V	E	T
SPYF-E_{I-II}	G	T	F	K	R

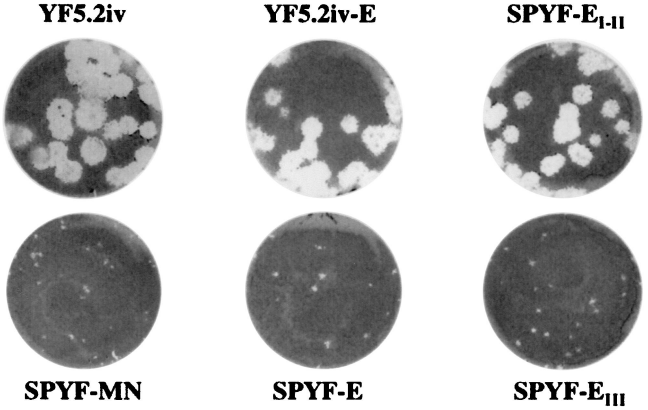

FIG. 2. Plaque sizes of engineered viruses. The parental and intratypic viruses were plaque purified on Vero cells for 6 days and stained for plaques as described in Materials and Methods.

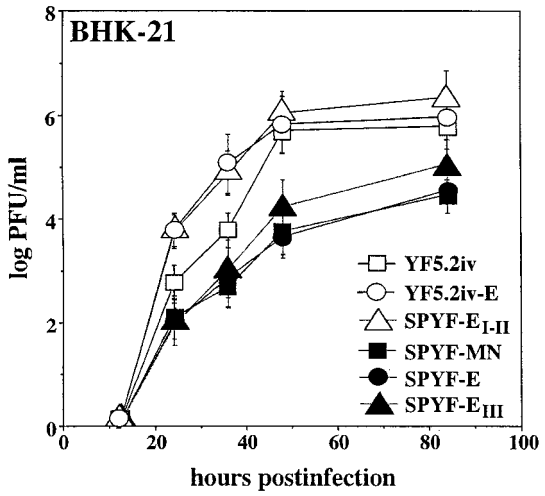

FIG. 3. Growth curves of parental and intertypic viruses on BHK-21 cells. Experiments were conducted as described in Materials and Methods, using multiplicities of infection of 0.001 PFU/cell. Samples were obtained in triplicate and titrated on Vero cells, and values indicate mean log PFU per milliliter ± standard errors of the means.

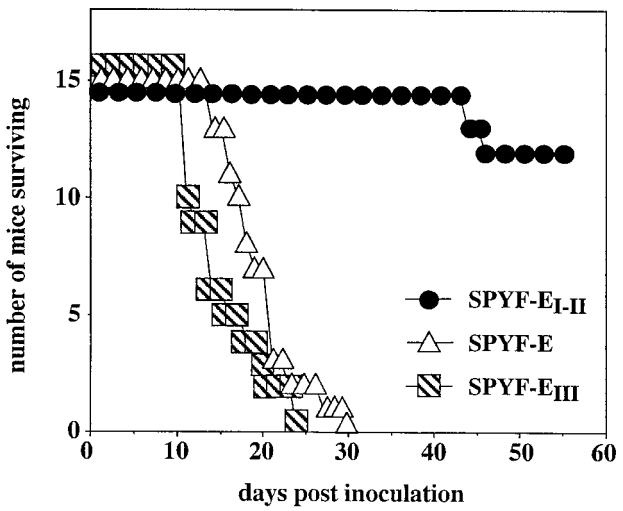

FIG. 5. Mortality data for SCID/ICR mice inoculated with 5×10^5 PFU of SPYF-E, SPYF-E_{I-II}, and SPYF-E_{III} viruses by the i.p. route. Experimental procedures were carried out as described in Materials and Methods. The mortality curves were constructed using data from three separate experiments for which similar survival times were recorded within groups of mice inoculated with the same viruses.

protein and that the nonstructural region of this virus may not independently contribute to this virulence effect, at least in the background of the YF5.2iv virus.

Neuroinvasiveness of SPYF-E_{III} and SPYF-E_{I-II} viruses. Because the initial experiments described above indicated that the SPYF-E virus contained the critical determinants of neuroinvasiveness for SCID mice, further investigation of the specific residues within the E protein which are involved in this phenotype was undertaken. Since domain III is believed to function as the cell receptor-binding region of the E protein, whereas domains I and II are primarily involved in the transition of the protein from a dimer to a fusion-active trimer (39, 46), we created two viruses in which the substitutions in domains I and II were segregated from those in domain III (Fig. 1). This approach would presumably give insight into whether the neuroinvasive properties are associated primarily with receptor-binding activity of the E protein or with subsequent events in virus entry. The SPYF-E_{III} virus contains SPYF-specific substitutions in domain III (residues 305, 326, and 380), whereas the SPYF-E_{I-II} virus contains SPYF-specific substitutions at positions 52 (domain II) and 173 (domain I) (Table 1). For both viruses, the remainder of the genome was derived from YF5.2iv. Figure 5 illustrates the results of testing in SCID/ICR mice, with SPYF-E virus used as a control for neuroinvasiveness. SPYF-E_{III} was highly neuroinvasive, causing 100% mortality, with an average survival time of 15.4 days (range, 11 to 24 days). This was similar to results with SPYF-E, for which the average survival time was 19.7 days in this experiment (range, 14 to 30 days). The difference in survival times between SPYF-E_{III} and SPYF-E was significant ($P < 0.02$). In contrast to these results, the SPYF-E_{I-II} virus was not highly neuroinvasive, with only 5 of 15 mice developing encephalitis, with an average survival time of 57.2 days (range, 44 to 77 days). These experiments show that the basis for high levels of neuroinvasiveness conferred by the SPYF E protein involves determinants in the receptor-binding domain III and that these high levels are not caused independently or redundantly by residues in domains I and II and/or the stem-anchor–transmembrane segment.

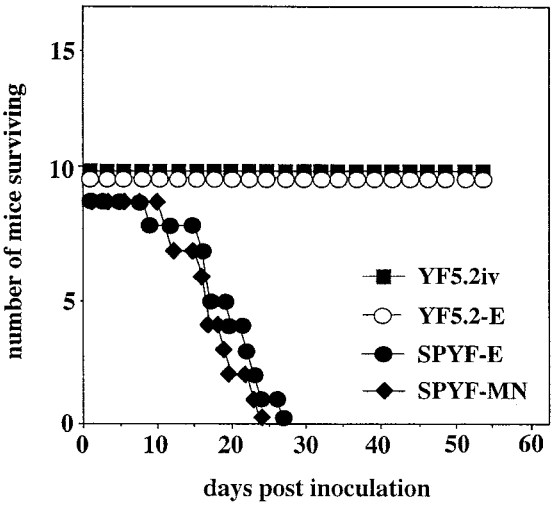

FIG. 4. Mortality data for SCID/ICR mice inoculated with 5×10^5 PFU of SPYF-MN, YF5.2iv, SPYF-E, and YF5.2-E viruses by the i.p. route. Experimental procedures were carried out as described in Materials and Methods. The mortality curves were constructed using data from two separate experiments for which similar survival times were recorded within groups of mice inoculated with the same viruses.

Virus burdens in tissues of mice. To further compare the virulence properties of the three engineered viruses which exhibited high levels of neuroinvasiveness (parental SPYF-MN, SPYF-E, and SPYF-E_{III}), tissue titration studies were performed on the mice which had succumbed to infection. The purpose was to determine if there were any differences in the distribution and extent of virus burdens at the time of fatal

TABLE 2. Virus burdens in SCID/ICR mice after peripheral inoculation

Virus	Virus burden (log PFU/g [± SEM])[a] in:									
	Serum[b]	Peritoneum	Heart	Lung	Muscle	Spleen	Liver	Kidney	Adrenal glands	Brain
SPYF-MN	3.2 (0.1)	2.4 (0.3)	1.1 (0.1)	2.4 (0.3)	2.0 (0.3)	1.8 (0.4)	0.62[c]	0.50 (0.1)	3.5 (0.4)	8.5 (0.4)
SPYF-E	3.3 (0.1)	2.4 (0.1)	1.5 (0.2)	2.1 (0.2)	2.5 (0.1)	2.0 (0.3)	0.95 (0.1)	0.64[c]	4.3 (0.3)	8.0 (0.2)
SPYF-E_{III}	2.7 (0.1)	2.5 (0.1)	1.2 (0.2)	2.0 (0.2)	2.7 (0.1)	1.6 (0.0)	0.65 (0.2)	0.40[c]	4.2 (0.1)	7.6 (0.2)
SPYF-$E_{I–II}$	2.5[c]	1.6 (0.9)	1.0[d]	2.1 (0.7)	2.9 (0.3)	3.0[c]	0.91 (0.4)	0.67[d]	5.3 (0.5)	7.5 (0.2)

[a] Data are titers based on groups of three to six mice, except as noted. Tissues were harvested at the time that individual mice exhibited signs of encephalitis.
[b] Data for serum are given as PFU per milliliter.
[c] $n = 2$.
[d] $n = 1$.

encephalitis. Results are shown in Table 2. There was a similar distribution of the three viruses in all peripheral tissues examined, based on the presence of measurable amounts of infectious virus by plaque assay. This method was sensitive for detection of even low levels of infectious virus (<1 log PFU/g of tissue) from these animals. The magnitudes of the virus burdens in different tissues were generally similar among the different virus groups. However, the highest burdens were observed in the central nervous system (CNS), where virus content ranged from 7.5 to 8.5 log (PFU/gram of brain). The levels of virus in sera were relatively similar among the different groups. Most other tissues contained quantities of titratable virus in the range of 2 to 4 log PFU/g. Mice infected with YF5.2iv virus were not included in these experiments, as it was previously shown that this virus replicates very poorly in comparison to SPYF-MN (8). Results are also shown for three mice infected with SPYF-E_{I-II} virus, who succumbed to infection at 44, 46, and 77 days postinoculation. The brains of these mice had slightly less virus than those of mice infected with the highly neuroinvasive viruses, and the peripheral tissues were less often positive for titratable virus, although the titers were sometimes higher (liver, adrenal glands, and spleen), presumably reflecting the longer period of virus replication in mice infected with SPYF-E_{I-II} than in mice that succumbed to the more neuroinvasive strains. The plaque sizes of the viruses recovered from brains of mice infected with SPYF-E_{I-II} virus were similar to that of the virus inoculated, suggesting that there was no mutation to a virus with the phenotype of SPYF-E_{III}. We did not test tissues of YF5.2iv-infected mice at times equivalent to those for SPYF-E_{I-II}-infected mice, and such studies are required to determine if there are absolute differences in survival and tissue burdens for YF5.2iv and SPYF-E_{I-II} viruses in this model, which would suggest an effect of the SPYF-MN substitutions at residues 52 and 173 on the virulence phenotype. These data indicate that there are no major differences in the tropisms and patterns of spread of the highly neuroinvasive viruses in the SCID mouse. This suggests that the E protein of SPYF virus confers a high level of infectivity on YFV for mouse tissues rather than merely conferring an increased level of neuroinvasiveness after i.p. inoculation.

Nucleotide sequencing of brain-associated SPYF viruses. We reported previously that SPYF-MN and its parental SPYF virus differed in neuroinvasiveness for normal mice, with the former not causing fatal neuroinvasiveness in 3-week-old mice and the latter causing 75% mortality in 3-week-old mice and 40% mortality in 5-week-old mice (8). These results were somewhat surprising in view of the similar neuroinvasive properties of these two viruses for SCID/ICR mice and suggested that SPYF-MN might be a quasispecies variant of SPYF virus. For instance, nucleotide substitutions in the E protein or elsewhere in the genome of SPYF-MN compared to SPYF might reduce its overall replicative fitness and limit its neuroinvasive properties in normal mice. In particular, the presence of the glutamate residue at position 326 of the E protein in the SPYF-MN clone, compared to the presence of a lysine residue at this position in other virulent YFV strains as well as the YF5.2iv virus, was suspected to be a deleterious substitution.

To further investigate this issue, we analyzed nucleotide sequences of viruses recovered from the brains of ICR mice which had succumbed to neuroinvasive disease with the parental SPYF virus (8). The population sequence of PCR products spanning the entire genome was determined for one such sample, and the E region and 3′ UTRs for viruses from three other mice were determined (Table 3). The complete genomic sequence matched that of the SPYF-MN clone except for two substitutions in the 3′ UTR (positions 10,508 and 10,631). Notably, the E regions were identical, and in particular, glutamate at position 326 rather than lysine was identified in the population sequence of SPYF virus. These same observations were also made for the E and 3′-UTR regions of viruses recovered from the other three mice. Thus, at the population level, SPYF-MN differs from the more neuroinvasive parental SPYF virus only in the 3′ UTR.

The nucleotide substitutions among the 3′ UTRs for YF5.2iv, SPYF-MN, and SPYF viruses were examined for their possible effects on predicted RNA secondary structures of the plus-strand RNA. Initially, a 3′-UTR structure for

TABLE 3. Nucleotide substitutions in YFV 3′ UTRs

3′ UTR nucleotide no.	Nucleotide in virus			Location[a]
	YF5.2iv	SPYF-MN	SPYF	
10,508	G	G	U	YF17D repeat 3, invariant hairpin 1
10,555	A	G	G	Dimorphic region I, disrupted hairpin 11
10,631	U	C	U	Conserved region II, invariant hairpin 4

[a] Location of substitutions refers to putative RNA structures as described in references 36 and 41. Sequences for YF5.2iv and SPYF-MN are based on the molecular clones for these viruses (40, 41). Sequences for SPYF are based on the population sequence obtained on viral RNA isolated from brains of ICR mice.

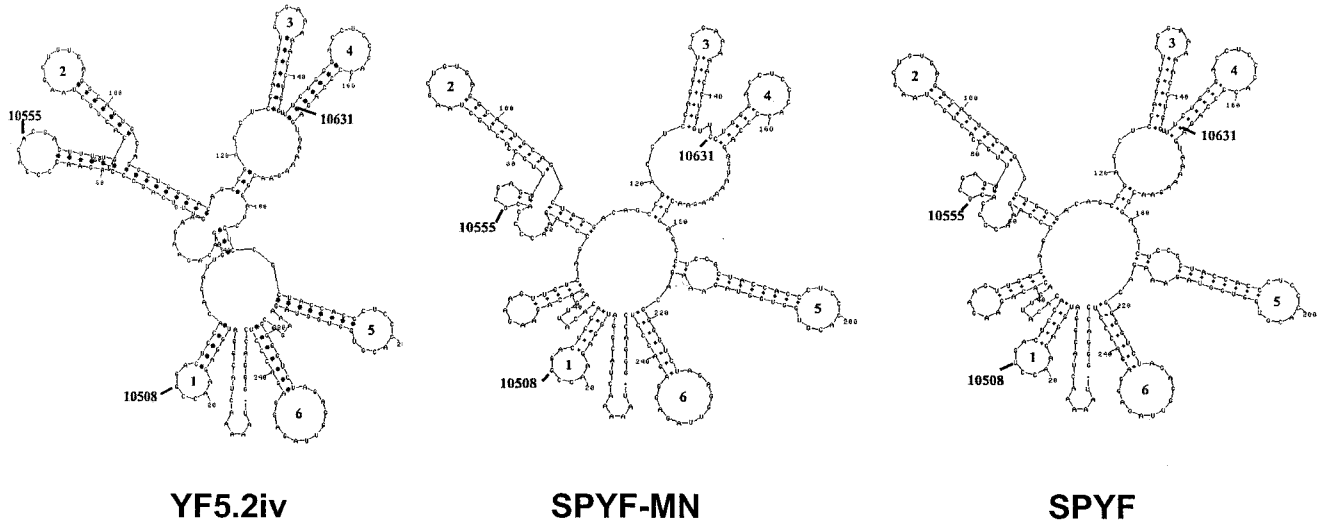

FIG. 6. Predicted RNA structures of the 3′ UTRs of the plus-strand RNAs for YF5.2iv, SPYF-MN, and SPYF viruses. The structures were generated as described in Materials and Methods. The positions of nucleotide substitutions which differentiate these three viruses are indicated. The conserved hairpins as defined for the 3′ UTRs of YFVs (36) are designated 1 through 6.

YF5.2iv was analyzed for compatibility with the structures predicted for the YFV 17D-204 strains (36, 37, 38), using parameters which permitted formation of the conserved stem and hairpin structures (hairpins 1, 2, and 6 in regions I and II as defined by Proutski et al. [36]). YF5.2iv and YFV 17D-204 differ by two nucleotide substitutions over the region analyzed (nt 10620 and 10681); however, at least two very similar structures with favorable energies were generated for these two viruses (data not shown). Structures for SPYF-MN and SPYF were then generated for comparison (Fig. 6). The SPYF-MN structure was constrained for formation of hairpins 1, 5, and 6, but not 2, 3, and 4, where the substitutions differing from YF5.2iv occur (nt 10555 and 10631). This resulted in the formation of a small branching hairpin proximal to loop 2, presumably as a result of the nt 10555 substitution. The substitution at nt 10631 was associated with truncation of the stem of hairpin 4 in SPYF-MN. Furthermore, elongation of the stem of hairpin 5 and formation of a proximal bulge loop were noted. A structure for SPYF was generated that was constrained only by formation of loops 5 and 6, allowing comparison to SPYF-MN for possible effects of nt 10508 and 10631 on their respective hairpins as well as the intervening regions. The structure differed from that of SPYF-MN by restoration of the length of stem 4 and constriction of the proximal branching bulge loop (nt 119 to 177) to exactly match YF5.2iv in this region, but it was otherwise indistinguishable. In particular, there was no obvious effect associated with substitution at position 10508. The SPYF-MN and SPYF viruses both exhibited an elongated stem-loop 5, with its proximal bulge, despite having the same nucleotide at position 10631. This suggests that nt 10555 is involved in the altered structure of stem-loop 5. A range of alternative structures for the three viruses were analyzed that had relatively similar energies and were constrained by the absence of base pairing among the initial 13 nt and between nt 15 through 18 and 183 through 186, both of which were required to optimize the YF5.2iv structure to that of YFV 17D-204 (36). These alternative structures lacked one or more of the predicted conserved hairpins 1 through 6, and no general consistency was apparent among them. These data suggest that the 3′ UTRs of SPYF-MN and SPYF differ from YF5.2iv in two regions of predicted conserved structure among YFV 17D strains, whereas SPYF-MN differs from SPYF in one conserved region.

DISCUSSION

YFV 17D, like some of the other neurotropic members of the *Flavivirus* genus, undergoes neuroadaptation during serial passage in mouse brain tissue, and this results in greater neurovirulence in this host, based on increased mortality rates, reduced average survival times, and a higher virus burden in the brain (8, 44). This phenotype is associated with the accumulation of multiple mutations in the viral genome that are presumably acquired sequentially as viral fitness for replication in the mouse CNS increases. In previous work, we identified the nucleotide substitutions which occur in the genome of YFV 17D as a result of this neuroadaptation (8, 44) and demonstrated that virus engineered to contain the nucleotide substitutions (the SPYF-MN clone) does in fact exhibit increased neurovirulence as well as increased neuroinvasiveness relative to nonneuroadapted YF5.2iv virus (8). SCID mice infected with SPYF-MN virus had readily detectable virus burdens in peripheral organs, which indicates that the mutations in its genome confer a generalized increase in infectivity for mouse tissues, not merely for the neurons within the CNS. Since mutations which increase the pathogenic potential of YFV in the context of the YFV 17D vaccine are undesirable, we sought to evaluate whether all or only some of the mutations in the neuroadapted SPYF-MN virus were required for its increased virulence phenotype in the SCID mouse model. The rationale for this investigation is based on the premise that the vaccine phenotype of the YFV 17D strain is likely to be of greater stability if multiple nucleotide substitutions are necessary to revert the virus to a high level of neurovirulence. The available

data on YFV 17D-associated encephalitis in humans suggest that neurovirulence can be increased by as few as one or two mutations in the E protein (18). However, it is possible that multiple pathways, involving either the E protein or other regions of the viral genome, exist for reversion of this virus. In this study, we engineered YFV 17D to contain substitutions which were naturally selected during the process of neuroadaptation. We therefore expect the data to be relevant to understanding the viral genetic basis for vaccine-associated encephalitis, although we acknowledge that there are important differences between the pathogenesis of this disease in mice and humans (32).

The results of our investigation indicate that the E protein is a critical factor for the neuroinvasive phenotype of YFV 17D in the SCID mouse model, despite the presence of candidate virulence determinants in multiple other regions of the SPYF-MN genome. Numerous other studies have implicated the E protein as a virulence factor for flaviviruses, based on observations that mutations within this protein affect neuroinvasive and neurovirulence phenotypes in the mouse model (7, 24, 33, 34, 42, 43; reviewed in reference 29). In various studies, molecular determinants within domains I, II, and III as well as the stem-anchor region have been shown to govern the functional activities of the E protein which are associated with virus entry into susceptible cells and which presumably contribute to pathogenesis (1, 2, 16, 46). With regard to the SPYF E protein, we evaluated the importance of five candidate virulence determinants (residues 52, 173, 305, 326, and 380) that are distributed through the three different domains. Residue 52 occurs in domain II at a site where mutations have been shown to influence the efficiency of cell penetration of Japanese encephalitis (JE) virus and also to affect neurovirulence of this virus in mice (15). Residue 173 occurs in domain I and is a determinant of a wild-type YFV-specific monoclonal antibody epitope (42). Substitutions at this position have been shown to abolish the epitope and to affect the mouse neurovirulence of the YFV 17D strain, with a threonine residue at this position acting as a virulence determinant (42). The role of substitutions at positions 52 and 173 of the SPYF E protein during neuropathogenesis in the mouse is not clear at the present time, since they did not exhibit a dominant effect in the SCID mouse model. However, effects of these substitutions might be more important during virus replication in the CNS, based on the fact that they were in fact selected during serial passage in mouse brains. Further studies are needed to evaluate the importance of the substitutions for efficiency of virus growth in the mouse CNS. In contrast to residues 52 and 173, residues 326 and 380 lie within the putative receptor-binding domain III, occupying a region of its lateral surface which is likely to be involved in interactions between the E protein and cell surface receptors (5). For instance, a substrain-specific epitope of YFV 17D has been shown to involve amino acid residue 325, and amino acid substitutions at this site can alter mouse neurovirulence (43). Residue 305 has also been implicated in the formation of the epitope; however, substitution at this position exhibited a subdominant effect on neurovirulence (43). Residue 380 is part of the RGD motif of mosquito-borne flaviviruses, and substitutions at this site in Murray Valley encephalitis virus (MVE) and YFV have been shown to affect the efficiency of virus spread in cell culture and to modulate neuroinvasion in mice (22, 48). It is becoming clear from various studies that multiple substitutions in the different domains of the flavivirus E protein may act coordinately to affect the function of this protein and hence may be collectively involved during the pathogenesis of encephalitic disease in the mouse model, presumably at the level of virus entry. In at least one model, there was a graded effect of mutations in the E protein on virulence properties, as lethality of chimeric YF/JE virus increased in proportion to the number of candidate virulence residues introduced into the JE virus E protein (3). However, these effects were observed in the context of a neurovirulence assay, and the contribution of E protein determinants to neuroinvasive properties may be different and not dependent on effects of multiple residues (29). It is also important to emphasize that the effects of attenuating substitutions in the E protein can be markedly influenced by covarying strain-specific genetic differences in this protein, at least in the context of mouse models of neurovirulence and neuroinvasiveness (42, 43).

Residues 305, 326, and 380 within domain III of the SPYF E protein were also observed to influence the cell culture properties of all viruses containing this region, which include the parental SPYF-MN virus, SPYF-E, and SPYF-E_{III}. All of these viruses exhibited a small plaque morphology on Vero cells and were impaired in replication kinetics compared to YFVs containing domain III of the YF5.2iv virus. Based on the very low multiplicities of infection used in the growth experiments, this suggests that the basis for the small plaque size and reduced replication efficiency involves a defect in cell-to-cell spread mediated by domain III of the SPYF virus. This may be a consequence of the alteration in local structure of the lateral surface of domain III caused by substitutions of glutamate at residue 326 and threonine at residue 380, such that interactions with cell surface receptors are compromised. The local structure is predicted to involve engagement of the side chains of these residues in multiple hydrogen bond formations with the main chain structure as shown in Fig. 7. For Glu_{326}, these include bonds between its carboxyl oxygen molecules and the main chain nitrogen molecule of Ser_{325} and the hydroxyl group as well as the main chain oxygen molecule of Thr_{301}. For Thr_{380}, bonds are predicted between its side chain hydroxyl group and the main chain oxygen molecule of Asp_{302} and between its main chain nitrogen molecule and the main chain oxygen molecules of Asp_{302} and Val_{337}. Arg_{380} in the SPYF E protein is predicted to form bonds between its main chain nitrogen molecule and the main chain oxygen molecules of Asp_{302} and Val_{378} as well as between its side chain nitrogen molecule and the main chain oxygen molecule of Lys_{303}. These predictions suggest that Arg_{380} and Lys_{326} are less constrained by local interactions and can adopt a configuration favorable for interaction of their side chains with solvent. Another consideration is that the loss of net positive charge resulting from the Glu_{326} and Thr_{380} substitutions is expected to reduce affinity for glycosaminoglycans, which might restrict cell-to-cell spread as a result of less-efficient interactions with these substances during early events in virus attachment. In this regard, the infectivity of YFV for cells in culture has been reported to be sensitive to inhibition by heparin, although the exact binding motifs on the E protein which are involved in this effect have not been characterized (14). A reduced affinity for glycosaminoglycans might also be a factor involved in the high

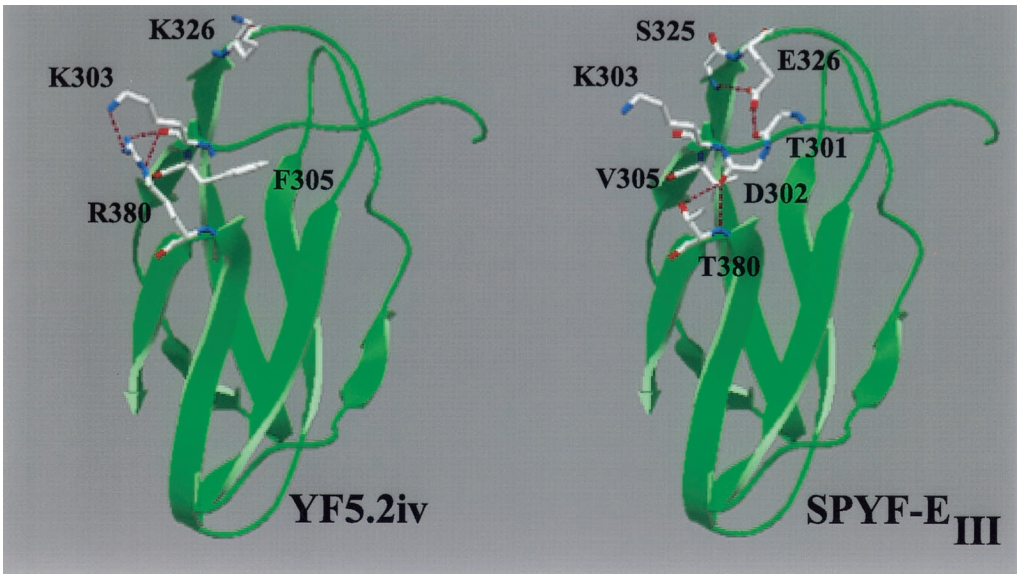

FIG. 7. Homology-based model of domain III of the YFV E protein based on the tick-borne encephalitis virus E protein. Substitutions at positions 305, 326, and 380 were modeled with respect to the most favorable energy configurations for side chain rotamers. Dashed lines indicate predicted hydrogen bond formations as described in the text.

level of neuroinvasiveness of SPYF-MN, SPYF-E, and SPYF-E_{III} viruses, as this property has been correlated with a lack of clearance of neuroinvasive strains of MVE and JE virus from the circulation in the mouse model (20) and with virulence of tick-borne encephalitis virus (25). Further experiments with the neuroadapted YFVs are required to determine whether reduced glycosaminoglycan binding is also a marker for high levels of neuroinvasiveness in the SCID mouse model and whether there is an independent effect causing increased infectivity for cells supporting permissive infection.

Various studies have suggested that molecular determinants involved in the functions of the nonstructural proteins also influence the virulence phenotypes of flaviviruses (6, 11, 19). Furthermore, comparison of the sequences of Asibi, French neurotropic vaccine, French viscerotropic, and SPYF-MN viruses reveals that some silent nucleotide substitutions are common to these three viruses (8). Although such substitutions could represent a selection for proteins and RNA structures which are required for efficient replication efficiency or for adaptation to host cells in vivo, our data suggest that in the SCID model of neuroinvasion, such substitutions are unlikely to have dominant effects on neuroinvasiveness. For instance, the nonstructural region of the SPYF-MN virus, when tested in the context of the YF5.2iv virus, did not appear to contribute any virulence effects above the level of the corresponding region of YF5.2iv virus. There are a total of 20 nt substitutions and 8 amino acid substitutions which differentiate the nonstructural proteins of these two viruses, including amino acid substitutions in the NS1, NS2A, NS4A, NS4B, and NS5 proteins. It is also possible that the nonstructural region of SPYF-MN encodes viral functions that act synergistically with the structural proteins of this virus for replication efficiency and/or virulence properties, and this would not be evident from analysis of the properties of the YF5.2-E virus. However, determination of the complete sequence of the parental SPYF virus which was highly neuroinvasive for 3-week-old mice revealed differences from SPYF-MN and also from YF5.2iv in the 3′ UTR (Table 3). Comparison of predicted RNA structures for the 3′ UTRs of these viruses revealed that both SPYF-MN and SPYF differed from YF5.2iv in the region immediately proximal to the conserved hairpin 2, where the branching loop structure of its rooting stem is disrupted. This corresponds to a structural difference noted between wild and vaccine strains of YFV (36), suggesting that it may be involved in conferring virulence properties upon YFVs. Comparison of SPYF-MN and SPYF revealed a difference only in the shape of hairpin 4. This structure appears to be conserved among all YFVs examined (36), and the fact that SPYF and YF5.2iv are identical with respect to this structure is consistent with this observation. It is possible that substitution at nt 10631 in the 3′ UTR of the SPYF-MN clone, which is associated with the aberration in hairpin 4, results in a deleterious effect upon viral replication that compromises the overall replication efficiency of SPYF-MN virus. In this regard, the high neuroinvasiveness of the SPYF parent may in part be dependent on a U at nucleotide position 10631, which may be more favorable for virus replication. The presence of the substitution at position 10508 between SPYF and SPYF-MN, while not affecting the structure of invariant hairpin 1, could also conceivably affect functional properties if, for instance, the loop is involved in RNA-protein interactions during viral RNA replication. The hypotheses concerning the importance of the 3′-UTR substitutions are currently being evaluated by engineering the SPYF-MN virus to contain the 3′ UTR of its parental SPYF virus or the YF5.2iv virus and by testing the neuroinvasiveness properties of the corresponding viruses in SCID/ICR and ICR mice.

The enhanced neurovirulence of neuroadapted YFV 17D was previously shown to involve the generation of higher titers of SPYF virus in the brain than what is achieved by YF5.2iv at

the same time after infection (44). This could also be primarily dependent on the effects of the E protein in increasing infectivity for neurons. It remains possible that the mutations we identified in the nonstructural protein regions of the SPYF-MN genome confer an enhanced replication efficiency upon YFV during infection of these cells. Direct comparisons of the growth efficiencies in the mouse CNS of the intertypic YFVs studied for the present report are needed to determine the relative contributions of the SPYF E protein alone versus those of the nonstructural region and 3′ UTR of this virus to enhanced growth efficiency in this compartment. At present, the effects of either of these regions might be expected to result in more rapid accumulation of virus burden in the CNS and a shortened incubation period for fatal encephalitis, perhaps involving neuronal apoptosis (10). Further studies with the mouse model described in this paper might also be useful to gain insight into reversion pathways of YFV 17D vaccine that involve mutations in the E protein or other regions of the genome. A better understanding of this phenomenon may be of benefit for evaluation of the attenuation properties of live-virus vaccines for flaviviruses produced by genetic engineering of molecular clones.

ACKNOWLEDGMENTS

This work was supported by grants from the NIH (AI-37646) and the Edward Mallinckrodt, Jr., Foundation.

REFERENCES

1. **Allison, S. L., J. Schalich, K. Stiasny, C. W. Mandl, C. Kunz, and F. X. Heinz.** 1995. Oligomeric rearrangement of tick-borne encephalitis virus envelope proteins induced by an acidic pH. J. Virol. **69:**695–700.
2. **Allison, S. L., K. Stiasny, K. Stadler, C. W. Mandl, and F. X. Heinz.** 1999. Mapping of functional elements in the stem-anchor region of tick-borne encephalitis virus envelope protein E. J. Virol. **73:**5605–5612.
3. **Arroyo, J., F. Guirakhoo, S. Fenner, Z.-X. Zhang, T. P. Monath, and T. J. Chambers.** 2001. Molecular basis for attenuation of neurovirulence of a yellow fever/Japanese encephalitis virus chimera vaccine (ChimeriVax-JE). J. Virol. **75:**934–942.
4. **Barrett, A. D. T., and E. A. Gould.** 1986. Comparison of neurovirulence of different strains of yellow fever virus in mice. J. Gen. Virol. **67:**631–637.
5. **Bhardwaj, S., M. Holbrook, R. E. Shope, A. D. T. Barrett, and S. J. Watowich.** 2001. Biophysical characterization and vector-specific antagonist activity of domain III of the tick-borne flavivirus envelope protein. J. Virol. **75:**4002–4007.
6. **Butrapet, S., C. Y.-H. Huang, D. J. Pierro, N. Bhamarapravati, D. J. Gubler, and R. M. Kinney.** 2000. Attenuation markers of a candidate dengue type 2 vaccine virus, strain 16681 (PDK-53), are defined by mutations in the 5′ noncoding region and nonstructural proteins 1 and 3. J. Virol. **74:**3011–3019.
7. **Chambers, T. J., A. Nestorowicz, P. W. Mason, and C. M. Rice.** 1999. Yellow fever/Japanese encephalitis chimeric viruses: construction and biological properties. J. Virol. **73:**3095–3101.
8. **Chambers, T. J., and M. Nickells.** 2001. Neuroadapted yellow fever virus 17D: genetic and biological characterization of a highly mouse-neurovirulent virus and its infectious molecular clone. J. Virol. **75:**10912–10922.
9. **Collier, W. A., H. De Roever-Bonnet, and J. Hoekstra.** 1959. A neurotropic variety of the vaccine strain 17D. Trop. Geogr. Med. **11:**80.
10. **Despres, P., M.-P. Frenkiel, P.-E. Ceccaldi, C. D. Dos Santos, and V. Deubel.** 1998. Apoptosis in the mouse central nervous system in response to infection with mouse-neurovirulent dengue viruses. J. Virol. **72:**823–829.
11. **Dunster, L. M., H. Wang, K. D. Ryman, B. R. Miller, S. J. Watowich, P. D. Minor, and A. D. T. Barrett.** 1999. Molecular and biological changes associated with HeLa cell attenuation of wild-type yellow fever virus. Virology **261:**309–318.
12. **Fitzgeorge, R., and C. J. Bradish.** 1980. The *in vivo* differentiation of strains of yellow fever virus in mice. J. Gen. Virol. **46:**1–13.
13. **Freestone, D. S.** 1994. Yellow fever vaccine, p. 741–779. *In* S. A. Plotkin and E. M. Mortimer (ed.), Vaccines, 2nd ed. W. B. Saunders, Philadelphia, Pa.
14. **Germi, R., J.-M. Crance, D. Garin, J. Guimet, H. Lortat-Jacob, R. W. H. Ruigrok, J.-P. Zarski, and E. Drouet.** 2002. Heparan sulfate-mediated binding of infectious dengue virus type 2 and yellow fever virus. Virology **292:**162–168.
15. **Hasegawa, H., M. Yoshida, T. Shiosaka, S. Fujita, and Y. Kobayashi.** 1992. Mutations in the envelope protein of Japanese encephalitis virus affect entry into cultured cells and virulence in mice. Virology **191:**158–165.
16. **Heinz, F. X., K. Stiasny, G. Puschner-Auer, H. Holtzmann, S. L. Allison, C. W. Mandl, and C. Kunz.** 1994. Structural changes and functional control of the tick-borne encephalitis virus glycoprotein E by the heterodimeric association with protein prM. Virology **198:**109–117.
17. **Jennings, A. D., J. E. Whitby, P. D. Minor, and A. D. T. Barrett.** 1993. Comparison of the nucleotide and deduced amino acid sequences of the envelope protein genes of the wild-type French viscerotropic strain of yellow fever virus and the live vaccine strain French neurotropic vaccine strain derived from it. Virology **192:**692–695.
18. **Jennings, A. D., C. A. Gibson, B. R. Miller, J. H. Mathews, C. J. Mitchell, J. T. Roehrig, D. J. Wood, F. Taffs, B. K. Sil, S. N. Whitby, J. E. Whitby, T. P. Monath, P. D. Minor, P. G. Sanders, and A. D. T. Barrett.** 1994. Analysis of a yellow fever virus isolated from a fatal case of vaccine-associated encephalitis. J. Infect. Dis. **169:**512–518.
19. **Kawano, H., V. Rostapshov, L. Rosen, and C.-J. Lai.** 1993. Genetic determinants of dengue type 4 virus neurovirulence for mice. J. Virol. **67:**6567–6575.
20. **Lee, E., and M. Lobigs.** 2002. Mechanism of virulence attenuation of glycosaminoglycan-binding variants of Japanese encephalitis virus and Murray Valley encephalitis virus. J. Virol. **76:**4901–4911.
21. **Liprandi, F.** 1981. Isolation of plaque variants differing in virulence from the 17D strain of yellow fever virus. J. Gen. Virol. **56:**363–370.
22. **Lobigs, M., R. Usha, A. Nestorowicz, I. D. Marshall, R. C. Weir, and L. Dalgarno.** 1990. Host cell selection of Murray Valley encephalitis virus variants altered at an RGD sequence in the envelope protein and in mouse virulence. Virology **176:**587–595.
23. **Mandl, C. W., H. Holzmann, T. Meixner, S. Rauscher, P. F. Stadler, S. L. Allison, and F. X. Heinz.** 1998. Spontaneous and engineered deletions in the 3′ noncoding region of tick-borne encephalitis virus: construction of highly attenuated mutants of a flavivirus. J. Virol. **72:**2132–2140.
24. **Mandl, C. W., S. L. Allison, H. Holzmann, T. Meixner, and F. X. Heinz.** 2000. Attenuation of tick-borne encephalitis virus by structure-based site-specific mutagenesis of a putative flavivirus receptor binding site. J. Virol. **74:**9601–9609.
25. **Mandl, C. W., H. Kroschewski, S. L. Allison, R. Kofler, H. Holzmann, T. Meixner, and F. X. Heinz.** 2001. Adaptation of tick-borne encephalitis virus to BHK-21 cells results in the formation of multiple heparan sulfate binding sites in the envelope protein and attenuation in vivo. J. Virol. **75:**5627–5637.
26. **Mathews, D. H., J. Sabina, M. Zuker, and D. H. Turner.** 1999. Expanded sequence dependence of thermodynamic parameters improves prediction of RNA secondary structure. J. Mol. Biol. **288:**911–940.
27. **McMinn, P. C., E. Lee, S. Hartley, J. T. Roehrig, L. Dalgarno, and R. C. Weir.** 1995. Murray Valley encephalitis virus envelope protein antigenic variants with altered hemagglutination properties and reduced neuroinvasiveness in mice. Virology **211:**10–20.
28. **McMinn, P. C., R. C. Weir, and L. Dalgarno.** 1996. A mouse-attenuated envelope protein variant of Murray Valley encephalitis virus with altered fusion activity. J. Gen. Virol. **77:**2085–2088.
29. **McMinn, P. C.** 1997. The molecular basis of virulence of the encephalitogenic flaviviruses. J. Gen. Virol. **78:**2711–2722.
30. **Meers, P. D.** 1959. Adaptation of the 17D yellow fever virus to mouse brain by serial passage. Trans. R. Soc. Trop. Med. Hyg. **53:**445–457.
31. **Men, R., M. Bray, D. Clark, R. M. Chanock, and C.-J. Lai.** 1996. Dengue type 4 mutants containing deletions in the 3′ noncoding region of the RNA genome: analysis of growth restriction in cell culture and altered viremia pattern and immunogenicity in rhesus monkeys. J. Virol. **70:**3930–3937.
32. **Monath, T. P.** 1986. Pathobiology of the flaviviruses, p. 375–440. *In* S. Schlesinger and M. J. Schlesinger (ed.), The *Togaviridae* and the *Flaviviridae*. Plenum Press, New York, N.Y.
33. **Ni, H., and A. D. T. Barrett.** 1998. Attenuation of Japanese encephalitis virus by selection of its mouse brain membrane receptor preparation escape mutants. Virology **241:**30–36.
34. **Ni, H., K. D. Ryman, H. Wang, M. F. Saeed, R. Hull, D. Wood, P. D. Minor, S. J. Watowich, and A. D. T. Barrett.** 2000. Interaction of yellow fever virus French neurotropic vaccine strain with monkey brain: characterization of monkey brain membrane receptor escape variants. J. Virol. **74:**2903–2906.
35. **Pletnev, A. G., M. Bray, and C.-J. Lai.** 1993. Chimeric tick-borne encephalitis and dengue type 4 viruses: effects of mutations on neurovirulence in mice. J. Virol. **67:**4956–4963.
36. **Proutski, V., M. W. Gaunt, E. A. Gould, and E. C. Holmes.** 1997. Secondary structure of the 3′-untranslated region of yellow fever virus: implications for virulence, attenuation and vaccine development. J. Gen. Virol. **78:**1543–1549.
37. **Proutski, V., E. A. Gould, and E. C. Holmes.** 1997. Secondary structure of the 3′ untranslated region of flaviviruses: similarities and differences. Nucleic Acids Res. **25:**1194–1202.
38. **Rauscher, S., C. Flamm, C. W. Mandl, F. X. Heinz, and P. F. Stadler.** 1997. Secondary structure of the 3′-noncoding region of flavivirus genomes: comparative analysis of base pairing probabilities. RNA **3:**779–791.
39. **Rey, F. A., F. X. Heinz, C. Mandl, C. Kunz, and S. C. Harrison.** 1995. The

envelope glycoprotein from tick-borne encephalitis virus at 2 angstrom resolution. Nature **375:**291–298.

40. **Rice, C. M., E. M. Lenches, S. R. Eddy, S. J. Shin, R. L. Sheets, and J. H. Strauss.** 1985. Nucleotide sequence of yellow fever virus: implications for flavivirus gene expression and evolution. Science **229:**726–733.
41. **Rice, C. M., A. Grakoui, R. Galler, and T. J. Chambers.** 1989. Transcription of infectious yellow fever virus RNA from full-length cDNA templates produced by *in vitro* ligation. New Biol. **1:**285–296.
42. **Ryman, K. D., H. Xie, T. N. Ledger, G. A. Campbell, and A. D. T. Barrett.** 1997. Antigenic variants of yellow fever virus with an altered neurovirulence phenotype in mice. Virology **230:**376–380.
43. **Ryman, K. D., T. N. Ledger, G. A. Campbell, S. J. Watowich, and A. D. T. Barrett.** 1998. Mutation in a 17D-204 vaccine substrain-specific envelope protein epitope alters the pathogenesis of yellow fever virus in mice. Virology **244:**59–65.
44. **Schlesinger, J. J., S. Chapman, A. Nestorowicz, C. M. Rice, T. E. Ginocchio, and T. J. Chambers.** 1996. Replication of yellow fever virus in the mouse central nervous system: comparison of neuroadapted and nonneuroadapted virus and partial sequence analysis of the neuroadapted strain. J. Gen. Virol. **77:**1277–1285.
45. **Schlesinger, R. W.** 1980. Virus-host interactions in natural and experimental infections with alphaviruses and flaviviruses, p. 83–104. *In* R. W. Schlesinger (ed.), The togaviruses. Academic Press, New York, N.Y.
46. **Stiasny, K., S. L. Allison, A. Marchler-Bauer, C. Kunz, and F. X. Heinz.** 1996. Structural requirements for low-pH-induced rearrangements in the envelope glycoprotein of tick-borne encephalitis virus. J. Virol. **70:**8142–8147.
47. **Theiler, M.** 1951. The virus, p. 46–136. *In* G. K. Strode (ed.), Yellow fever. McGraw-Hill, New York, N.Y.
48. **van der Most, R. G., J. Corver, and J. H. Strauss.** 1999. Mutagenesis of the RGD motif in the yellow fever virus 17D envelope protein. Virology **265:**83–95.
49. **Vlaycheva, L. A., and T. J. Chambers.** 2002. Neuroblastoma cell-adapted yellow fever 17D: characterization of a viral variant associated with persistent infection and decreased virus spread. J. Virol. **76:**6172–6184.
50. **Wang, E., K. D. Ryman, A. D. Jennings, D. J. Wood, F. Taffs, P. D. Minor, P. G. Sanders, and A. D. T. Barrett.** 1995. Comparison of the genomes of the wild-type French viscerotropic strain of yellow fever virus with its vaccine derivative French neurotropic vaccine. J. Gen. Virol. **76:**2749–2755.
51. **Zuker, M., D. H. Mathews, and D. H. Turner.** 1999. Algorithms and thermodynamics for RNA secondary structure predictions: a practical guide, p. 11–43. *In* J. Barciszewski and B. F. C. Clark (ed.), RNA biochemistry. NATO ASI Series. Kluwer Academic Publishers, Boston, Mass.